AF2009164

Eighth USA/Europe Air Traffic Management Research and Development Seminar (ATM2009)

A Comparison of Algorithm Generated Sectorizations

Shannon Zelinski
System Modeling and Optimization Branch
NASA Ames Research Center
Moffett Field, California, USA
Shannon.J.Zelinski@nasa.gov

***Abstract*— This paper compares several algorithm generated airspace boundary designs, known as sectorizations. Three algorithms are chosen that approach the airspace sectorization problem in different ways. Due to the disparity in their methods, they produce radically different looking sectorizations. Simulations of air traffic operating in each of the sectorizations is completed and their resulting demand, capacity, complexity, and delay metrics are compared. All three algorithm generated sectorizations suggested possible improvements in system efficiency and workload balancing over today's operations.**

Keywords-airspace design; capacity management; dynamic airspace configuration

NOMENCLATURE

i	=	flight index
k	=	quarter-hour index
s	=	sector index
r	=	region comprised of a group of sectors
$t_e(s,i)$	=	flight i egress time from sector s
$t_i(s,i)$	=	flight i ingress time into sector s
$t_u(i)$	=	flight i unconstrained gate arrival time
$t_c(i)$	=	flight i constrained gate arrival time
$N_f(s)$	=	the set of all flights within sector s between 7AM and 7PM local time
$N_f(r)$	=	the set of all flights flying through region r
$N_s(r)$	=	the set of all sectors in region r
$n_f(s)$	=	total number of flights in set $N_f(s)$
$n_f(r)$	=	total number of flights in set $N_f(r)$
$n_s(r)$	=	total number of sectors in set $N_s(r)$
$c(s)$	=	capacity (MAP value) for sector s
$\delta(s)$	=	average time a flight spends in sector s
$m(s,k)$	=	average flight count in sector s for quarter-hour k
$m(s)$	=	average flight count in sector s between 4PM and 12AM UTC
$M(r)$	=	average $m(s) \forall s \in N_s(r)$
$\sigma_m(r)$	=	standard deviation of $m(s) \forall s \in N_s(r)$
$\Sigma_c(r)$	=	sum of $c(s) \forall s \in N_s(r)$
$C(r)$	=	average $c(s) \forall s \in N_s(r)$
$\sigma_c(r)$	=	standard deviation of $c(s) \forall s \in N_s(r)$
$\rho(s)$	=	flight count/capacity ratio for sector s
$P(r)$	=	average $\rho(s) \forall s \in N_s(r)$
$\sigma_\rho(r)$	=	standard deviation of $\rho(s) \forall s \in N_s(r)$
$\epsilon(r)$	=	average total delay for all flights in region r
$R_\epsilon(r)$	=	recovered average total delay for region r
$R_t(r)$	=	recovered average throughput for region r
$[x_1 ... x_7]$	=	array of 7 complexity components
$[w_1 ... w_7]$	=	array of 7 complexity weight coefficients
$\chi(s,k)$	=	sector s complexity for quarter-hour k
$\chi(s)$	=	average $\chi(s,k)$ for 4PM-12AM UTC
$X(r)$	=	average $\chi(s) \forall s \in N_s(r)$
$\sigma_\chi(r)$	=	standard deviation of $\chi(s) \forall s \in N_s(r)$
subscripts		
d	=	demand, unconstrained
t	=	throughput, constrained

I INTRODUCTION

Several algorithms have been developed for repartitioning airspace into sectors given a set of flight tracks. Each algorithm attempts to laterally partition a layer of airspace to minimize and/or balance controller workload. They approach the problem in different ways and produce sectors that are different.

Previous analyses assessed algorithmic success at a regional scale using different historical flight track data. Reference [1] compares a current day sectorization with those generated from two different algorithms. Reference [2] evaluates sectorizations generated from a single algorithm using different optimization functions. Both analyses are constrained to the Fort-Worth Center and compare aircraft-count metrics based on historical flight track data. Because of their use of historical flight track data only, there have been no analyses performed for expected future traffic levels. Thus far, a number of algorithms, including those cited above, have been developed but their relative value is not known at a national scale or for future traffic levels.

This paper assesses the relative value of several algorithms for future traffic levels on the national level. That is, a side-by-side comparison using the same flight track data examined the comparative value of each algorithm. Also, in addition to considering current traffic levels, simulations at 1.5 time todays

traffic level were conducted. These simulations expanded the previous area of consideration from the regional level to the entire continental United States airspace.

This paper is organized as follows. Section II presents an overview of the sectorization algorithms. The experiment design is presented in section III. Section IV describes the metrics used to compare the sectorizations. Section V discusses results. Finally, concluding remarks are presented in section VI.

II Sectorization Algorithms

This section presents an overview of the three algorithms used to produce sectorizations.They all try to produce a sectorization that minimizes or balances a workload metric while conforming to traffic flows. The main objective function, method of conforming to flows, and method for determining the number of sectors are described for each.

A Flight Clustering Algorithm

The Flight Clustering algorithm[3] groups flight tracks together to sectorize airspace. It is constrained to a maximum specified number of flight tracks per cluster. Sector boundaries are then formed around the clusters. This limits the amount of workload required to control a sector.

The clustering algorithm approach allows Dynamic Density[11] metrics to be implicitly manipulated. It attempts to partition airspace in such a manner that acceptable Dynamic Density levels are achieved, and the impact on user-preferred flight routes is minimized. Flight route segments are clustered according to distances of clustering criteria from the cluster center. These criteria are selected and weighted to achieve control over the Dynamic Density of the resulting airspace partition.

1) Objective Function: The flight clustering objective is to minimize the sum of the 'distance' metric between flight tracks and the assigned cluster center based on the selected clustering distance criteria. The clustering criteria include current and future distance, lateral and vertical speed, and heading. Another clustering criteria, referred to as the 'Corridor' criteria, includes the perpendicular distance of the flight position from the major axis of the group of flight positions associated with the cluster and the flight's heading difference with respect to the major axis. All the above clustering criteria were used for this experiment.

2) Flow Conformance: All of the clustering criteria attempt to group flight tracks that belong to the same flow, especially the corridor criteria.

3) Number of Sectors: The number of sectors is determined by a user defined target number-of-flight-tracks-per-cluster parameter. Flight tracks are clustered into groups within a minimum and maximum threshold of the target number.

B Voronoi Genetic Algorithm

The Voronoi Genetic algorithm[2] uses a Voronoi Diagram to partition the airspace and a genetic algorithm to optimize the partitions.

The Voronoi Diagram decomposes a space into subdivisions around given generating points. All coordinates within a region associated with a specific generating point are closer to that generating point than any other generating point.

The genetic algorithm is a guided random search based on the principals of genetic inheritance and Darwinian evolution. Here, the genetic algorithm is used to find the set of Voronoi Diagram generating points that optimize given parameters. This algorithm can use any number of objective funtions.

1) Objective Function: For this experiment, the genetic algorithm objective function is to maximize a capacity estimate minus peak aircraft count of each sector. The capacity estimate for each sector is directly related to the average flight time through that sector.

2) Flow Conformance: Because the capacity estimate for each sector is directly related to the average flight time through that sector, sectors with longer average flight times will have higher capacity and work toward the objective function. Sectors with longer average flight times also tend to align to major flows.

3) Number of Sectors: The number of resulting sectors is determined by the number of Voronoi Diagram generating points chosen to partition a region of airspace. Assuming a goal average capacity of 15 aircraft per sector, the desired number of sectors for a given region is estimated by dividing the peak traffic count for the region by 15.

C Mixed Integer Programming Algorithm

The Mixed Integer Programming (MIP) algorithm[4] discretizes the airspace into hexagonal cells and clusters the cells according to workload and connectivity. The workload of a cell is the number of flight track counts within that cell. Connectivity from cell i to a neighboring cell j is the total number of fights that travel from cell i to the cell j. Thus, connectivity is an abstract quantity of workload flow. Flow enters each cell from at least one of it's neighbors and exits into exactly one neighboring cell. The workload of each cell is added to the flow, which is finally absorbed by a sink cell. A sector consists of all cells whose flows converge to one sink. Potential sink cells are chosen at random.

Improvements to the MIP algorithm were made in [5] by making connectivity between cells symmetric. By redefining the connectivity between two neighboring cells i and j to include both flights traveling from cell i to cell j and from cell j to cell i, flows become bidirectional and give the optimization more options to find a feasible solution with a lower objective function.

1) Objective Function: The MIP objective function is to balance the total number of flights tracks of a cluster of cells while minimizing the connectivity between cells in different clusters.

2) Flow Conformance: Becasue the algorithm attempts to

minimize the flow between cells in different sectors, the cell clusters will tend to be oriented along the dominant traffic flows

3) Number of Sectors: The number of resulting sectors is determined *a priori*.

III Experiment Design

This section discusses how the experiment was designed. The goal was to perform a side-by-side comparison of the current day sectorization and several algorithm generated sectorizations for the continental US airspace. Therefore, each sectorization is generated according to the same guidelines using the same flight track data.

Rather than using historical data to evaluate the sectorizations, flight track data is generated through simulation to remove the effects of current sector constraints and traffic management initiatives. Simulating the flight track data also allows the sectorizations to be evaluated for projected future traffic levels that do not exist in historical data.

Simulations were completed using the Airspace Concept Evaluation System (ACES) [6]. ACES models gate-to-gate flight operations on airport surfaces and in terminal and enroute airspaces. These include gate pushback and arrival, taxi, runway takeoff and landing, local approach and departure, climb, decent, transition, and cruise. Air traffic control and traffic flow management models control flights during these operations to ensure that airport and airspace capacity constraints are not violated.

Fig. 1 shows the process used to generate sectors, estimate capacities, and simulate traffic for each algorithm. Each of the stages in this process are discussed in the following subsections.

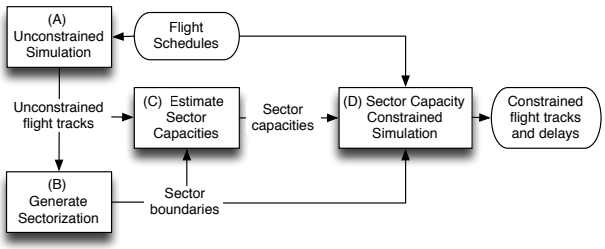

Figure 1: Experiment process.

A *Unconstrained Simulation*

The first stage of the experiment process is to simulate unconstrained flight tracks. The unconstrained simulation flies each flight without any airport or sector capacity constraints according to it's flight plan contained in the flight schedule.

The flight schedule consisted of all the flight plans departing within 24 hours from a single high-traffic, good-weather day starting at 4/21/2005 8AM GMT. The last flight plan submitted before departure for each flight was used. The unconstrained simulation produced flight tracks for every minute of each flight. These flight tracks were used to generate new sectorizations with new sector capacities.

B *Generating Sectorizations*

The second stage of the experiment process generates new sectorizations using the unconstrained flight tracks produced by the first stage. Due to the infinite number of ways each sectorization algorithm could generate new airspace partitions, the algorithms are made to follow guidelines that make the resulting sectorizations more comparable. These are described below.

The algorithms all produce lateral airspace divisions for a given set of flight track data. The current airspace sectorization is far more complicated than a single layer of sectors spanning the nation. First, national airspace is divided into regions called centers, and then, it is subdivided into sectors. Sectors are also stratified into low, high, and super-high altitudes. Sectors within the same stratum may have different altitude ranges.

Future airspace operational concepts do not necessarily preclude the airspace from being redesigned irrespective of center boundaries. However, in order to make the sectorization comparable at a more regional level, all sectorization algorithms were constrained to redesigning the airspace within the current center boundaries shown in Fig. 2.

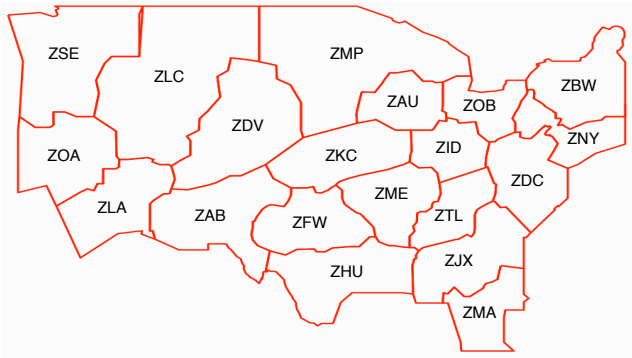

Figure 2: Continental United States airsapce centers.

Separate sectorizations were created for a high-altitude airspace layer, occupying flight levels 240 through 350 (23,950 to 35,050 feet), and a super-high-altitude layer, occupying flight levels 351 and above (over 35,050 feet). Airspace below 23,950 feet was not redesigned.

A current day sectorization from 2005 was modified to be comparable with the algorithm generated sectorizations. By design, sectors were already organized within centers, but altitude ranges were not consistent between altitude stratum. To ensure that at least the same overall volume of airspace was compared, the 2005 sectorization was truncated below 23,950 feet. All sectors with a maximum altitude greater than 23,950 feet were given a minimum altitude of 23,950 feet. Any sector with a minimum altitude of 23,950 feet was classified as high altitude, and any sector that did not have another sector above it was classified as super-high altitude. Some sectors covered the entire

altitude range and were classified as both high and super-high altitude sectors, even though they were not split.

C Estimating Sector Capacities

After new sectorizations were generated, their sector capacities were estimated. Several methods for estimating sector capacity have been proposed in the literature [7, 8]. However, the most straightforward capacity estimation method, and the one used for this experiment, is the method used by the FAA to determine Monitor Alert Parameter (MAP) values [9]. The MAP formula is a function of the average flight time of aircraft in the sector between 7AM and 7PM local time.

$$\delta(s) = \frac{1}{n_f(s)} \sum_i (t_e(s,i) - t_i(s,i)) \forall i \in N_f(s) \quad (1)$$

$$c(s) = \begin{cases} 5 & \text{if} \quad \frac{5}{3}\delta(s) \leq 5 \\ \frac{5}{3}\delta(s) & \text{if} \quad 5 < \frac{5}{3}\delta(s) < 18 \\ 18 & \text{if} \quad \frac{5}{3}\delta(s) \geq 18 \end{cases} \quad (2)$$

These equations were used to calculate $c(s)$ for all high and super-high altitude sectors in a current day sectorization from 2005 and for each of the new sectorizations. The FAA allows $c(s)$ to be adjusted nominally +/- 3 when needed based on the judgment of traffic management representatives. Therefore, the $c(s)$ values calculated for the 2005 sectorization are different from their published MAP values.

D Constrained Simulation

The final stage of the experiment process is to simulate constrained flight tracks for each sectorization. Constraints are applied to airport and sector capacities in an ACES simulation. Air traffic control and traffic flow management models control flights to ensure that capacity constraints are not violated by delaying flights along their filed flight plan. For the purposes of this experiment, only capacity constraints on sectors within redesigned airspace are applied. Airport capacities and capacities for airspace outside the scope of this experiment are left unconstrained. The sector capacity constrained simulations result in a unique set of constrained flight track data for each sectorization simulated. These flight tracks and simulated delays are used to generate metrics with which to compare the sectorizations.

IV Metrics

This section discusses the metrics used to compare the sectorizations. All of the metrics can be applied to a group of sectors. The basic metrics are number of sectors, demand, throughput, capacity, complexity, and delay. The demand/capacity and throughput/capacity ratios are also of interest because ideally, capacity should be placed where demanded.

A Number of Sectors

There were no restrictions made on the number of sectors, $n_s(r)$, generated for a given region r in the new sectorizations. Everything else being equal, a lower n_s is desirable to make more efficient use of controller resources. There is an inherent tradeoff between n_s and capacity. As $n_s(r)$ increases, the sum capacity in r would be expected to increase as well. However, increasing n_s reduces the average sector size which may make average $\delta(s)$ and $c(s)$ for each sector lower. At some point, increasing the number of sectors will reduce average sector capacity so much that the sum capacity of the sectors does not increase.

B Demand and Throughput

Demand and throughput metrics are based on average instantaneous sector flight counts within quarter-hour intervals. Demand and throughput are computed from unconstrained and constrained flight track data, respectively. Demand and throughput metrics are computed for a region of airspace, r, by averaging the average instantaneous flight counts per quarter-hour over the mid 8 hours of the day when traffic is highest. A region can comprise any group of sectors, such as a single sector, center, altitude layer, or NAS-wide. Let $m(r,k)$ be the average flight count in r for quarter-hour, k. The average sector flight count in r is given by

$$m(r) = \frac{1}{32} \sum_{k=k_0}^{k_0+32} m(r,k). \quad (3)$$

Let the subscripts d and t denote demand and throughput. Let $M_d(r)$ and $M_t(r)$ be the average $m_d(s)$ and $m_t(s)$ for all s in r. Let $\sigma_{m_d}(r)$ and $\sigma_{m_t}(r)$ be the standard deviations for $m_d(s)$ and $m_t(s)$ for all s in r.

Throughput is desired to be as close as possible to demand. The ratio of throughput to demand should be as close to 1 as possible. Recovered throughput is a metric designed to evaluate how much a new sectorization increases the throughout/demand ratio from the Current Day sectorization. Let $R_t(r)$ be the recovered average throughput in region r given by

$$R_t(r) = 1 - \frac{m_d(r) - m_t(r)}{m_{d0}(r) - m_{t0}(r)} \quad (4)$$

where the subscript 0 denotes the Current Day sectorization.

Assuming that maximum quarter-hourly flight count is a major component of controller workload, it is desirable for $\sigma_{m_d}(r)$ and $\sigma_{m_t}(r)$ to be low in order to balance the workload.

C Capacity

The capacity of each sector is defined according to (1) and (2). The $c(s)$s are used as constant constraints for the sector capacity constrained ACES simulations. Capacity sum, average, and standard deviation for regions or sectors are computed as well. Let $\Sigma_c(r)$, $C(r)$, and $\sigma_c(r)$ be the sum, average, and standard deviation of $c(s)$ for all s in r.

Higher $\Sigma_c(r)$ and $C(r)$ are desirable to enable increased throughput. Intuitively, a lower $\sigma_c(r)$ should be desirable. However, capacities themselves are designed to keep workload within acceptable limits. Therefore, there may be a tradeoff between balancing workload metrics and capacity. It is more desirable to balance workload metrics than capacity.

D Capacity Ratios

A set of metrics that is perhaps more relevant than demand and throughput, or capacity, are the ratios of demand and throughput to capacity. Ideally, capacity should be placed where the demand is in order to maximize overall throughput. The demand/capacity ratio is a measure of how well the sectors accommodate the traffic, and the throughput/capacity ratio is a measure of workload levels.

Let $\rho_d(s)$ and $\rho_t(s)$ be the average maximum quarter-hourly demand/capacity and throughput/capacity ratios for s over the mid 8 hours of the day given by

$$\rho_d(s) = \frac{m_d(s)}{c(s)} \quad (5)$$

$$\rho_t(s) = \frac{m_t(s)}{c(s)}. \quad (6)$$

Average and standard deviations of capacity ratios for regions of sectors are also computed. Let $P_d(r)$ and $P_t(r)$ be the average $\rho_d(s)$ and $\rho_t(s)$ for all s in r. Let $\sigma_{\rho_d}(r)$ and $\sigma_{\rho_d}(r)$ be the standard deviations of $\rho_d(s)$ and $\rho_t(s)$ for all s in r.

E Complexity

There has been a lot of research done to develop complexity metrics that measure controller workload [10, 11, 12, 13, 14, 15]. These efforts concentrate on identifying and validating up to 52 quantifiable complexity variables based on the factors that contribute to workload. References [13], [14], and [15] present the most simplified subset of complexity metrics referred to as Simplified Dynamic Density (SDD) metrics. SDD metrics comprise just seven components that can be derived from historical track data. The combined SDD metric was chosen to represent complexity in this experiment.

The seven components (x_1 through x_7) of SDD are occupancy count, proximity, altitude transition, sector boundary crossing, aircraft per sector volume, heading variance, and cruise speed variance. These are calculated per quarter-hour and are combined in a weighted sum. Component weights were taken from [15]. Each component is described below.

1) Occupancy Count (x_1) and Aircraft per Sector Volume (x_5): The occupancy count component for SDD metrics is the average instantaneous sector flight count for the given quarter-hour. Therefore, $x_1(s,k) = m(r,k)$ where $N_s(r) = \{s\}$. Aircraft per sector volume is simply x_1 divided by the sector volume in cubic kilometers.

2) Proximity (x_2): Proximity events of different severity levels are calculated for all aircraft pairs within 10 nmi. Proximity severity levels in [13], [14], and [15] were designed to account for location uncertainty, time-stamps being recorded at different times, and one minute granularity. The proximity severity computations for simulation data have been simplified with respect to time, because the one minute time-stamps for each flight are produced for the exact same time. Table I shows the criteria for calculating proximity severity level between a pair of aircraft within the same time-stamp.

TABLE I: PROXIMITY SEVERITY LEVEL CRITERIA

Severity Level	Vertical Sep.	Horizontal Sep.
1	<1000 ft	<5 nmi
2	<1000 ft	5 to 7.5 nmi
3	<1000 ft	7.5 to 10 nmi
4	≥1000 ft	<5 nmi

The combined proximity component, $x_2(s,k)$, is defined as follows.

$$x_2(s,k) = \frac{1}{4}(4p_1 + 2p_2 + p_3 + p_4) \quad (7)$$

where p_1, p_2, p_3, and p_4 indicate the number of proximities counted in s during k for each corresponding severity level.

3) Altitude Transitions (x_3): Altitude transitions are counted for tracks that climb or descend more than 500 feet within a minute. $x_3(s,k)$ is the sum of all tracks within s during k that are not within 500 feet of their last track.

4) Sector Boundary Crossings (x_4): Every time a flight crosses a sector boundary, a boundary crossing is counted for both the outbound and inbound sector. $x_4(s,k)$ is the combined number of flights that enter or exit s within k.

5) Heading variance (x_6) and speed variance (x_7): Heading and speed variances, $x_6(s,k)$ and $x_7(s,k)$, are calculated for the set of tracks in sector s within k. Variances are calculated for heading in degrees and for groundspeed in knots.

6) Combined SDD Components: The seven SDD components described above were combined in a weighted sum as follows.

$$\mathbf{x} = [\mathrm{x}_1, \mathrm{x}_2, \mathrm{x}_3, \mathrm{x}_4, \mathrm{x}_5, \mathrm{x}_6, \mathrm{x}_7] \quad (8)$$

$$\mathbf{w} = [2.2, .4, .3, .5, 30000, .0005, .0005] \quad (9)$$

$$\chi = \mathbf{w} \cdot \mathbf{x}' \quad (10)$$

where $\mathbf{w}$ weights were taken from [15]. The average complexity for a given sector, $\chi(s)$, is calculated similar to $m(s)$ as follows.

$$\chi(s) = \frac{1}{32} \sum_{k=k_0}^{k_0+32} \chi(s,k) \quad (11)$$

where k_0 is the first quarter hour in the 8 hours for which s has the highest average traffic counts.

Average and standard deviations of complexity for regions of sectors are also computed. Let $X(r)$ be the average $\chi(s)$ for all s in r. Let $\sigma_\chi(r)$ be the standard deviation of $\chi(s)$ for all s in r.

F Delay

ACES collects the time for various events of each simulated flight. The difference between event times for unconstrained and constrained simulations is delay. Traffic flow management models may apply delay multiple times to the same flight in order to meet multiple constraints. Sector delays are computed

as average total delay for all flights flying through the sector. Delays by region are computed similarly.

The total delay for a single flight is the difference between it's constrained and unconstrained gate arrival time. Let $\epsilon(r)$ be the average total delay for all flights in region r given by

$$\epsilon(r) = \frac{1}{n_f(r)} \sum_i (t_c(i) - t_u(i)) \forall i \in N_f(r) \qquad (12)$$

where $t_c(i)$ and $t_u(i)$ are the constrained and unconstrained gate arrival times for flight i.

V Simulation Results

This section presents and discusses the metric comparison results between sectorizations. Each of the three algorithms used flight tracks generated from an unconstrained simulation of a current day traffic schedule (1X) to create unique sectorizations subject to the guidelines discussed in section III.B. Fig. 3 shows the resulting sectorizations for high altitude Fort Worth Center in black overlaying flight tracks in grey. The most notable difference between the sectorizations are the number of sectors. This will be discussed in section V.A below. Another notable difference is in boundary smoothness. The rough boundaries in the MIP sectorization are a result of the hex cell clustering method. All sectorizations tend to direct the major axis of their sectors toward the middle of the center. This follows the major flow patterns in and out of this center's largest airport located in the middle of the center.

The same set of unconstrained 1X flight tracks were used to estimate sector capacities for each of these sectorizations and the modified current day sectorization. These sector capacities were then used to simulate constrained 1X flight tracks through each sectorization.

In order to test the sectorizations with more futuristic flight traffic levels, a flight demand generation tool called AvDemand[16] was used to homogeneously grow the 1X flight traffic schedule to 1.5X. Another unconstrained simulation was used to generate unconstrained 1.5X flight tracks for this traffic schedule. No new sectorizations or capacity estimations were generated using the unconstrained 1.5X flight tracks. Instead, the 1X generated sectorizations and capacity estimations were used to simulate constrained 1.5X flight tracks.

The resulting 16 sets of flight track data were used to calculate the metrics defined in section IV. They consisted of 4 (sectorizations) by 2 (constrained and unconstrained) by 2 (1X and 1.5X). The following subsections discuss the compared results of these 16 sets of metrics.

A Number of Sectors

No design restriction for number of sectors for each region was placed on the sectorization algorithms. Therefore, some sectorizations resulted in very different numbers of sectors from the current day sectorization.

Fig. 4 shows each sectorization's total number of sectors for the National Airspace System (NAS), $n_s(\text{NAS})$, at each

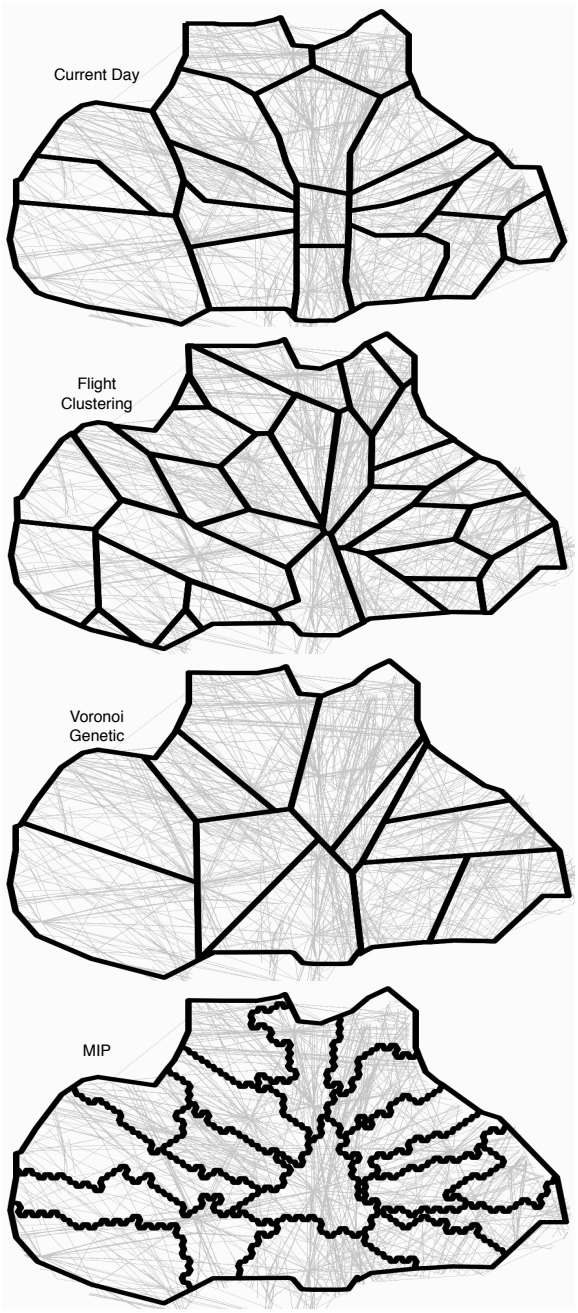

Figure 3: Traffic patterns and sectorizations for high altitude Fort Worth Center (ZFW).

altitude stratum. The NAS includes all 20 centers. For the algorithm generated sectorizations, $n_s(\text{NASall})$ is the sum of $n_s(\text{NAShigh})$ and $n_s(\text{NASsuper})$. This relationship does not hold for the current day sectorization becasue there were many sectors classified as both high and super-high altitude due to the inconsistent altitude structure. The MIP algorithm was given a goal number of sectors per center similar to the average number of sectors at any one altitude for that center. The MIP number of sectors is the same for both high and super-high altitude stratums. The number of sectors for the Flight Clustering and Voronoi Genetic sectorizations were influenced by other algo-

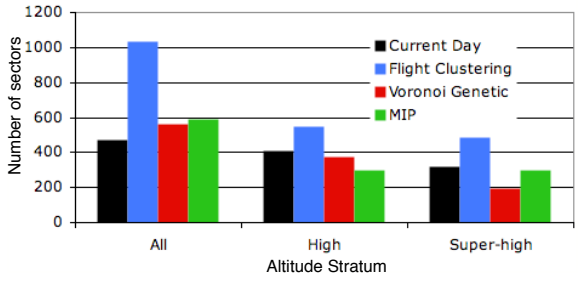

Figure 4: Total number of sectors in the National Airspace System, $n_s(\text{NAS})$, for each altitude stratum.

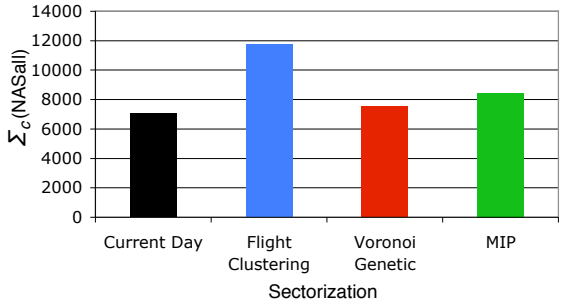

Figure 5: Sum capacity in the National Airspace System, $\Sigma_c(\text{NASall})$, for each sectorization.

rithm parameters as described in sections II.A and II.B. Both resulted in fewer super-high sectors than high sectors. All the algorithm generated sectorizations have more total sectors than the current day sectorization, perhaps because of the NAS-wide altitude stratification design guideline. The Flight Clustering produced more than twice as many total sectors. If number-of-flight-tracks-per-cluster parameter were increased, the resulting number of sectors would be decreased. A sensitivity analysis has not yet been completed to determine the optimal parameter setting.

The relative numbers of sectors per center for each sectorization follow similar patters as the NAS. There are several exceptions for high altitude centers where the Voronoi Genetic algorithm produces close to or more than the number of sectors as the Flight Clustering Algorithm. These centers are ZDC, ZID, ZNY, and ZOB, all busy centers.

B Capacity

Like number of sectors, capacity is something that is unique to each sectorization. Although 1X unconstrained track data was used to estimate the capacities of each sectioization, the same set of capacities was used in both the 1X and 1.5X constrained simulations.

In general, average capacities, $C(r)$, are lower for the algorithm generated sectorizations than the current day sectorization. However, because algorithm sectorization resulted in more sectors per region, the sum capacities, $\Sigma_c(\text{NASall})$, are higher than for the Current Cay sectorization, especially in the case of the Flight Clustering sectorization. Fig. 5 shows $\Sigma_c(\text{NASall})$ for each sectorization. The Flight Clustering and Voronoi Genetic algorithms show general increases in $\sigma_c(r)$ over Current Day, whereas the MIP algorithm shows general decreases in $\sigma_c(r)$ over Current Day. Consistency in capacity between sectors is not as important as constancy in capacity ratios or complexity discussed in later sections.

C Demand and Throughput

The demand and throughput metrics are important metrics for assessing how well the sectorization accommodates traffic demand. These metrics compare track data from unconstrained and constrained simulations within the same 1X or 1.5X traffic level. Fig. 6 and 7 show the NAS-wide average throughput/demand percentages for each altitude stratum for 1X and 1.5X traffic, respectively. Higher percentages indicate that the traffic is less constrained and throughput is being allowed to reach demand levels.

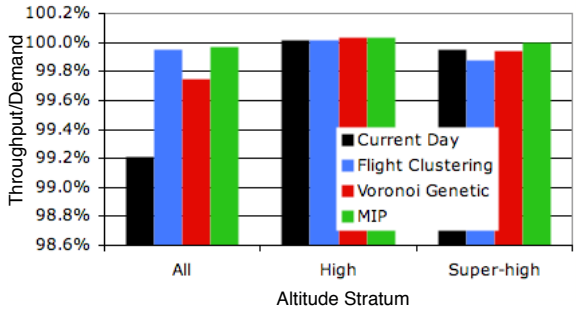

Figure 6: Average 1X Throughput/Demand in the National Airspace System, $\frac{m_t(\text{NAS})}{m_d(\text{NAS})}$, for each altitude stratum.

As seen in Fig. 6 for 1X traffic, the algorithm generated sectorization increases average NAS throughput/demand percentages, but there is very little room to improve because the Current Day sectorization 1X throughput/demand percentage is already above 99%. In some cases, the percentage is slightly above 100%. This is possible due to minor traffic schedule shifting, which causes more aircraft to occupy an airspace at the same time than was originally demanded.

The 1.5X traffic strains the system to more than the 1X traffic. It more effectively evaluates the algorithm generated sectorizations improvements over the Current Day sectorization. Fig. 7 clearly shows that all three algorithm generated sectorizations produce higher throughput/demand percentages than the Current Day sectorization. Flight Clustering and MIP sectorizations produce larger improvements at the high altitude stratum and the Voronoi Genetic algorithm produces the largest improvement at the super-high altitude stratum.

Fig. 8 shows the recovered throughput, $R_t(r)$, for both stratums combined at each region. For each algorithm generated sectorization, there are one to three centers with negative recovered throughout. These are instances where the throughput

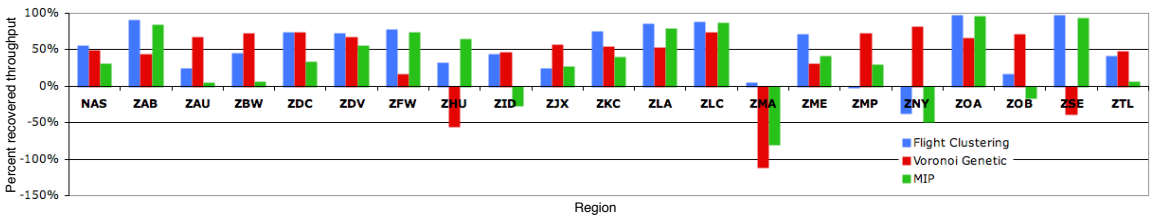

Figure 8: Percent recovered throughput by region, $R_t(r)$, for 1.5X traffic.

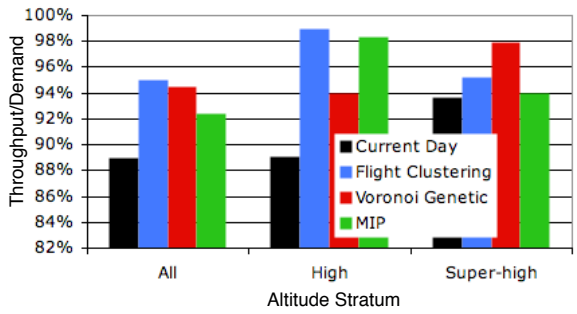

Figure 7: Average 1.5X Throughput/Demand in the National Airspace System, $\frac{m_t(\text{NAS})}{m_d(\text{NAS})}$, for each altitude stratum.

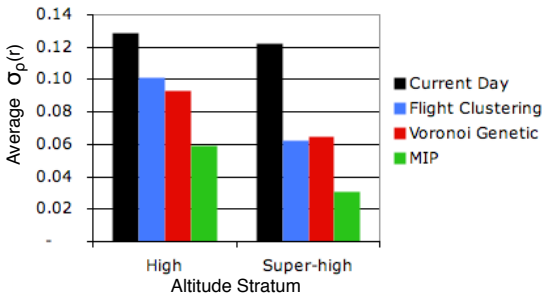

Figure 9: Average 1X standard deviation of Demand/Capacity for all center regions within each altitude stratum.

is lower than in the Current Day sectorization. This can happen in less busy centers when the $m_{d0}(r) - m_{t0}(r)$ term from Eqn. 4 is less than $m_d(r) - m_t(r)$. In each case, the sectorizations with negative throughput/demand percentage are the ones with the lowest number of sectors for the center.

D *Capacity Ratios*

The standard deviations of demand/capacity and throughput/capacity ratios between sectors in a region are more important that the ratios themselves. The standard deviations, especially for ρ_d as opposed to ρ_t, indicate whether capacity is distributed appropriately to accommodate demand. A smaller $\sigma_\rho(r)$ means that the sectorization placed more capacity where demand needed it, and less capacity where it wasn't needed. Because, each sectorization was design for a single center at a single stratum at a time, it makes the most sense to evaluate $\sigma_\rho(r)$ at the single center and stratum level.

Fig. 9 shows the average $\sigma_{\rho_d}(r)$ across all centers in each altitude stratum for each sectorization. All three algorithm generated sectorizations show a reduced average $\sigma_{\rho_d}(r)$ over the Current Day sectorization. The MIP algorithm does an especially good job of distributing capacity appropriately to match demand. It has half the average $\sigma_{\rho_d}(r)$ for high altitude and a quarter the average $\sigma_{\rho_d}(r)$ for super-high altitude.

The 1X average $\sigma_{\rho_t}(r)$s are almost identical to the 1X average $\sigma_{\rho_d}(r)$s . This is not surprising, considering how little throughput deviated from demand for all of the 1X simulations.

Both the average $\sigma_{\rho_d}(r)$s and $\sigma_{\rho_t}(r)$s for 1.5X show the exact same trend between sectorizations and altitude stratum as in Fig. 9. The the average $\sigma_{\rho_d}(r)$s increased by 70% and the average $\sigma_{\rho_t}(r)$s increased by 46% between 1X and 1.5X traffic levels. The percent increase in average $\sigma_{\rho_d}(r)$ is the same as the percent increase in $P_d(r)$. This indicates that the 1.5X flight tracks are a good representation of homogeneous 1.5X growth from the 1X flight tracks. The percent increase in average $\sigma_{\rho_t}(r)$ is a little lower than the percent increase in $P_t(r)$ due to the smoothing effect of delaying flights to meet the capacity constraints.

E *Complexity*

Complexity is computed to serve as a more realistic measure of controller workload than just occupancy count. All of the sectorization algorithms utilize metrics that relate to complexity components other than occupancy count. Although, occupancy count is still a driving factor in the design.

Fig. 10 shows the average NAS-wide complexity within each altitude stratum for 1X and 1.5X, and unconstrained and constrained simulations. Because occupancy count is a heavily weighted component of complexity, 1.5X has larger $X(\text{NAS})$s than 1X, and $X_t(\text{NAS})$ is lower than $X_d(\text{NAS})$ for every sectorization as occupancy counts are controlled to be below capacity contraints. $X_t(\text{NAS})$ is only slightly lower than $X_d(\text{NAS})$ for 1X because the throughput did not deviate from demand much at 1X.

The Flight Clustering sectorization reduces complexity the most due to it's high number of sectors and consequently low number of flights per sector. Other complexity components in-

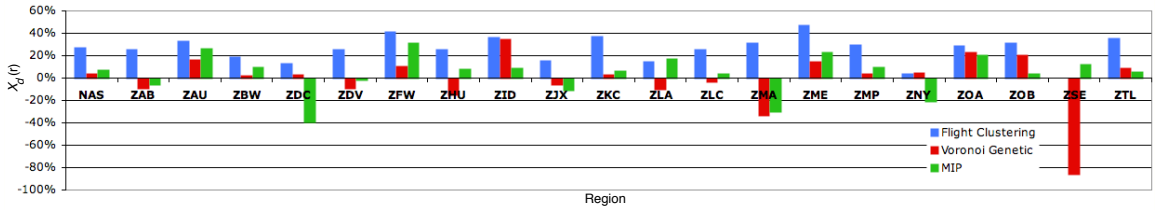

Figure 11: Percent that $X_d(r)$ is reduced from the Current Day to each algorithm generated sectorization by region for 1X traffic.

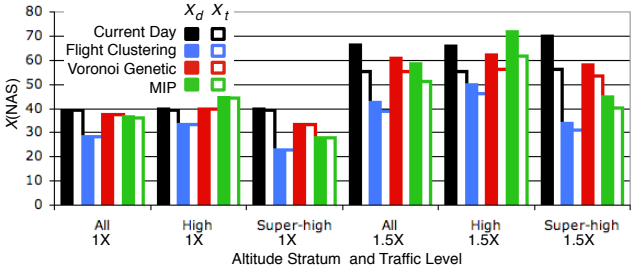

Figure 10: Average Complexity in the National Airspace System, $X(\text{NAS})$, within each altitude stratum.

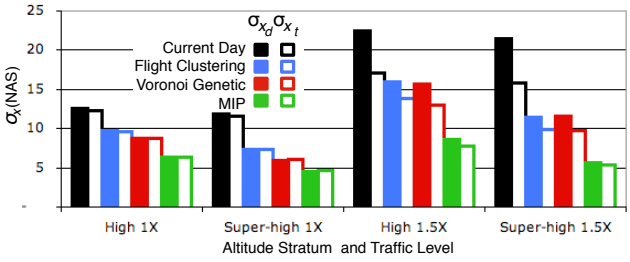

Figure 12: Average standard deviation of Complexity for all centers, $\sigma_\chi(\text{r})$, within each altitude stratum.

crease more for Flight Clustering due to the reduced average size of more sectors, but reduced occupancy count makes up for increases in other components. The Voronoi Genetic sectorization has the most similar $X(\text{NAS})$ between altitude stratums because number of sectors designed for each center and altitude stratum were based on the occupancy count. MIP is the only algorithm generated sectorization with higher $X(\text{NAS})$ than Current Day for the high-altitdue stratum. MIP also had the least number of sectors at this stratum.

Fig. 11 shows the percentage each algorithm generated sectorization reduces $X_d(r)$ from the Current Day sectorization at 1X broken out by center regions. The Flight Clustering sectorization is the only one that reduces $X_d(r)$ for every center. Many of the centers for which the Voronoi Genetic or MIP sectorization increase complexity are the same centers for which $R_t(r)$ was negative in Fig. 8. These were the centers with the lowest number of sectors.

Fig. 12 shows the average $\sigma_\chi(r)$ for all centers within each altitude stratum for 1X and 1.5X and unconstrained and constrained simulations. Average $\sigma_\chi(r)$ follows the same trend as $X(\text{NAS})$ between 1X and 1.5X and between unconstrained and constrained simulations. Super-high altitude average $\sigma_\chi(r)$s are consistantly lower than for High altitude.

Average $\sigma_\chi(r)$s are significantly lower for the algorithm generated sectorizations than the Current Day sectorization. The Flight Clustering and Voronoi Genetic sectorizations have very similar average $\sigma_\chi(r)$. The average $\sigma_\chi(r)$ for MIP is much lower in each case. This means that the MIP algorithm did the best job of distributing workload, as measured by SDD complexity, evenly between sectors.

F *Delay*

Delay is the ultimate measure of cost to the airspace system customers. Table II shows the average total delay simulated for all flights, $\epsilon(\text{NAS})$, at 1X and 1.5X traffic for each sectorization. All of the algorithm generated sectorizations significantly reduce delay by similar amounts. While delays are still reduced at 1.5X, the amount varies more by sectorization.

The Voronoi Genetic algorithm shows the most robust partitioning with respect to delay for increasing traffic demand. The Voronoi Genetic objective function directly affected delay by minimizing the possibility of traffic demand exceeding capacity constraints.

TABLE II: $\epsilon(\text{NAS})$ FOR EACH CONSTRAINED SIMULATION.

Sectorization	ϵ**(NAS) for 1X**	ϵ**(NAS) for 1.5X**
Current Day	3.99 min	45.02 min
Flight Clustering	0.39 min	18.68 min
Voronoi Genetic	0.47 min	16.50 min
MIP	0.55 min	30.11 min

Fig. 13 and 14 show the percent recovered delay, $R_\epsilon(r)$, for each center region. There were more instances of negative $R_\epsilon(r)$, indicating increased delay over the Current Day sectorization. This is because at many centers, the 1X traffic did not stress the system enough to incur significant delay, especially Cleveland Center (ZOB). ZOB is a very busy center for which the airspace was more recently designed than other centers to accommodate it's high demand. Only the MIP sectorization shows negative $R_\epsilon(r)$ at 1.5X for the same three centers with significant negative $R_\epsilon(r)$ at 1X.

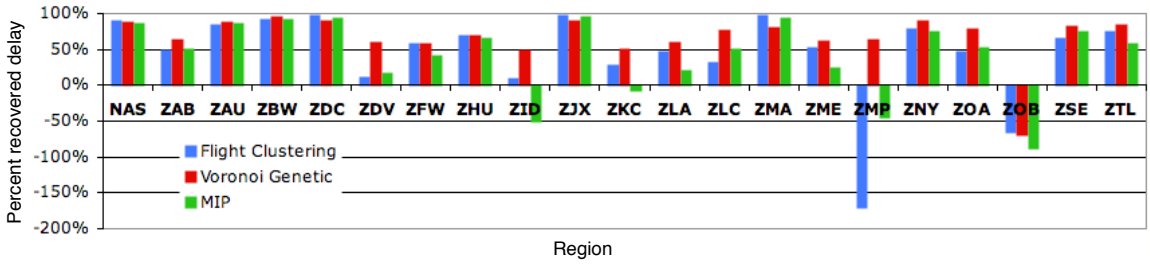

Figure 13: Percent recovered delay by region, $R_\epsilon(r)$, for 1X traffic.

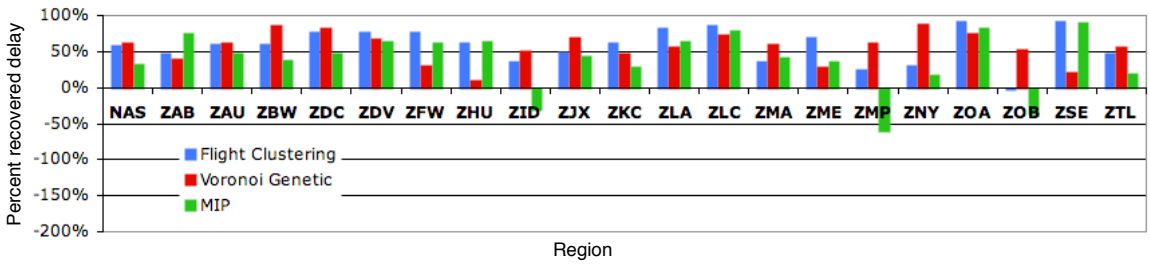

Figure 14: Percent recovered delay by region, $R_\epsilon(r)$, for 1.5X traffic.

G *Results Summary*

The benefits of new airspace configurations are expected to include improved system efficiency and more balanced controller workload. A few of the metrics discussed above, R_t and R_ϵ reflect system efficiency. σ_{χ_d} and σ_{ρ_d} reflect controller workload balance. These metrics, along with number of sectors, portray a summary of new sectorization benefits.

Table III shows the total number of sectors, system efficiency, and workload balancing metrics computed for the entire NAS for each sectorization with 1.5X traffic. The best result for each metric is underlined. Some of these metrics portray the sector benefits a little differently with respect to one another when altitude stratum are combined vs. when they are computed separately. All three algorithm generated sectorizations show improvements in all summary benefit metrics except number of sectors. Flight Clustering more than doubles the number of sectors. Voronoi Genetic and MIP methods have more comparable numbers of sectors to current day but still increase the total number. This may be due to the NAS-wide altitude stratification guideline. There are many areas of the NAS where a single stratum of sectors is used from above flight level 240, whereas algorithm generated sectorizations assumed two stratum. Flight Clustering and Voronoi Genetic show comparable benefits in both system efficiency and workload balancing metrics, but the Voronoi Genetic sectorization has a much more comparable number of sectors to current day than the Flight Clustering sectorization. MIP shows lower system efficiency gains than the other two sectorizations, but it is very good at balancing complexity and demand/capacity between sectors, while maintaining a comparable number of sectors to current day. Due to it's low number of sectors, most robust increases in system efficiency, and second best workload balancing, the Voronoi Genetic sectorization appears to be the best sectorization compared in this experiment.

TABLE III: NAS-WIDE SUMMARY METRICS FOR EACH SIMULATION WITH 1.5X TRAFFIC.

Sectorization	R_t	R_ϵ	σ_{χ_d}	σ_{ρ_d}	n_s
Current Day	–	–	16.8	0.22	<u>470</u>
Flight Clustering	<u>55%</u>	59%	13.4	<u>0.16</u>	1031
Voronoi Genetic	50%	<u>63%</u>	14.0	0.17	565
MIP	31%	33%	<u>12.5</u>	0.18	593

VI CONCLUSIONS

This experiment is the first US nationwide, side-by-side comparison of different algorithm-generated sectorizations. Simulating traffic through each of these sectorizations for a 1.5X traffic schedule improved the comparison by stressing the system enough to evaluate the algorithms strengths and weaknesses.

Each algorithm shows its strengths and weaknesses through the different metrics. The Flight Clustering sectorization significantly increased throughput, while reducing complexity and delay, but only at the cost of doubling the number of sectors that exist in today's system. The Voronoi Genetic sectorization had a more comparable number of sectors to today's system, while increasing throughput and reducing delay similar to the Flight Clustering algorithms. The Voronoi Genetic sectorization had a

more modest reduced complexity over the Current Day sectorization with respect to Flight Clustering. The MIP sectorization also had comparable numbers of sectors to Current Day with similar increases in throughput to Flight Clustering and Voronoi Genetic. However, the MIP algorithm's greatest strength was in balancing capacity and complexity. Overall, the Voronoi Genetic sectorization performed the best in this experiment.

Two major realizations from this experiment were that the number of sectors designed for each region and the altitudes at which airspace is stratified are not trivial airspace design factors. These design factors need to be better incorporated into the algorithms. The number of sectors has been well integrated in to the Flight Clustering design but sensitivity analyses still need to be performed to evaluate how the rest of the metrics are affected as the number-of-flight-tracks-per-cluster parameter is increased and the number of sectors decreases.

All three algorithm sectorization showed improved system efficiency and workload balancing over current day. This indicates that these sectorization methods have merit and are worth continued development and more detailed analysis.

ACKNOWLEDGMENT

Many thanks to Charlene Cayabyab for her above-and-beyond excellent support on this research in the ACES lab at NASA Ames Research Center.

REFERENCES

[1] Mitchell, J., Sabhnani, G., Krozel, J., Hoffman, B., and Yousefi, A. 2008. Dynamic Airspace Configuration management Based on Computational Geometry Techniques. In *AIAA Guidance, Navigation and Control Conference and Exhibit*, August, Honolulu, Hawaii. AIAA-2008-7225.

[2] Xue, M. 2008. Airspace Sector Redesign Based on Voronoi Diagrams. In *AIAA Guidance, Navigation and Control Conference and Exhibit*, August, Honolulu, Hawaii. AIAA-2008-7223.

[3] Brinton, C. and Pledgie, S. 2008. Airspace Partitioning Using Flight Clustering and Computational Geometry. In *27th Digital Avionics System Conference*, St. Paul, Minnesota.

[4] Yousefi, A., Khorrami, B., Hoffman, R., and Hackney, B. "Enhanced Dynamic Airspace Configuration Algorithms and Concepts, Metron Aviation Inc., Tech. Rep. Report No. 34N1207-001-R0, December 2007.

[5] Drew, M. 2008. Analysis of an Optimal Sector Design Method. In *27th Digital Avionics System Conference*, St. Paul, Minnesota.

[6] Meyn, L., Windhorst, R., Roth, K., Van Drei, D., Kubat, G., Manikonda, V., Roney, S., Hunter, G., Huang, A., and Couluris, G. 2006. Build 4 of the Airspace Concept Evaluation System. In *AIAA Modeling and Simulation Technologies Conference an Exhibit*, Keystone, CO. AIAA-2006-6110.

[7] Welch, J. 2007. Macroscopic Workload Model for Estimating En Route Sector Capacity. In *7th USA/Europe ATM R&D Seminar*, Barcelona, Spain.

[8] Song, L., Wanke, C., and Greenbaum, D. 2007. Predicting Sector Capacity for TFM. In *7th USA/Europe ATM R&D Seminar*, Barcelona, Spain.

[9] Federal Aviation Administration, Order JO 7210.3V, "Section 7. Monitor Alert Parameter," [online publication] URL: http://www.faa.gov/airports_airtraffic/air_traffic/publications/ATpubs/FAC/Ch17/s1707.html [cited 26 November 2008].

[10] Masalonis, A., Callaham, M., and Wanke, C. 2003. Dynamic Density and Complexity Metrics for Realtime Traffic Flow Management. In *5th USA/Europe ATM R&D Seminar*, Budapest, Hungary.

[11] Kopardekar, P. 2007. Airspace Complexity Measurement: An Air traffic Control Simulation Analysis. In *7th USA/Europe ATM R&D Seminar*, Barcelona, Spain.

[12] Lee, K., Feron, E., and Pritchett, A. 2007. Air Traffic Complexity: An Input-Output Approach. In *Proceedings of the 2007 American Control Conference*, July 11-13, New Youk City, New York.

[13] Klein, A., Rodgers, M., Lucic, P., and Leiden, K. 2008. "Airspace Complexity Metric for Dynamic Airspace Configuration: Simplified Dynamic Density (SDD)," unpublished.

[14] Rodgers, M., Lucic, P., Klein, A., and Leiden, K. 2008. "Dynamic Airspace Configuration Algorithms," unpublished.

[15] Klein, A., Rodgers, M., and Leiden, K. 2009. "Simplified Dynamic Density: a Metric for Dynamic Airspace Configuration and NEXTGEN Analysis," unpublished.

[16] Huang, A. and Schleicher, D. 2008. Futuristic US Flight Demand Generation Approach Incorporating Fleet Mix Assumptions. In *AIAA Modeling and Simulation Technologies Conference an Exhibit*, 18 - 21 August 2008, Honolulu, Hawaii. AIAA 2008-6678.

AUTHOR BIOGRAPHY

Shannon J. Zelinski received a M.S. degree in Electrical Engineering Robotics and Controls from the University of California at Berkeley in 2003. She then joined the Aviation Systems Division at NASA Ames Research Center, where she gained expertise in air traffic management, simulation validation, and future demand generation, working with the Airspace Concept Evaluation System. Ms. Zelinski currently leads Dynamic Airspace Configuration research at NASA as an Associate Principal Investigator for the NextGen-Airspace project.